International Journal of Thermophysics, Vol. 13, No. 4, 1992

The Thermal Conductivity of the Molten $NaNO_3$–KNO_3 Eutectic Between 525 and 590 K

R. M. DiGuilio[1] and A. S. Teja[1]

Received January 21, 1992

Molten salts are one of the few remaining classes of fluids for which standard-quality (±1% accuracy) data on thermal conductivity have not hitherto been available. We have therefore developed a new apparatus based on the transient hot-wire technique to obtain reference-quality measurements of the thermal conductivity of molten salts at high temperatures. Liquid metal-filled quartz capillaries served as insulated hot wires in our method, and in addition, a two-wire technique was used in order to obtain absolute values of the thermal conductivity. New data for the $NaNO_3$–KNO_3 eutectic between 525 and 590 K are reported in this paper and comparisons with other recent measurements are shown.

KEY WORDS: hot-wire technique; molten salt; thermal conductivity.

1. INTRODUCTION

Molten salts are finding increasing use as heat storage media, in fuel cells, and as media for the destruction of hazardous waste. As a result, knowledge of their thermophysical properties is becoming increasingly important in the design of equipment for these applications. However, measurement of the thermophysical properties of molten salts is difficult because of the high temperatures involved and the corrosive nature of these salts in the molten state. This is especially true in the case of thermal conductivity, for which standard-quality data (±1% accuracy) have hitherto been unavailable. Recently, Nagasaka and Nagashima [1] reviewed the data for the thermal conductivity of molten potassium and sodium nitrate and found that the data were in disagreement by as much as 40%. Disagreements among data sets are even higher for other substances. A technique for the measurement of the thermal conductivity of molten salts

[1] School of Chemical Engineering, Georgia Institute of Technology, Atlanta, Georgia 30332, U.S.A.

0195-928X/92/0700-0575$06.50/0

with an accuracy comparable to that available for other fluids (ca. 1%) is, therefore, of great interest. The transient hot-wire technique, commonly used for nonelectrolytes, is not directly applicable to electrolytes because the method relies on having an electrically heated wire immersed directly in the fluid whose thermal conductivity is to be measured. If the fluid itself conducts electricity, then measurement is not possible. The adaptation to electrically conducting fluids is simple in principle: the wire must be electrically insulated from the liquid. In practice, this is difficult to achieve, especially if measurements are to be made over a wide range of temperatures, because the insulating layer generally cracks or loses its insulative properties at high temperatures. Omotani et al. [2–4] pioneered a promising technique which uses a fine glass capillary filled with liquid metal as an insulated hot wire in measurements of the thermal conductivity of molten salts.

The purpose of this work was to develop an apparatus based on the transient hot-wire technique for measurement of the thermal conductivity of molten salts with an accuracy ($\pm 1\%$) characteristic of standard-quality thermal conductivity data [5]. The availability of a standard data set would make possible the assessment of other data, the testing of models, and the calibration of new thermal conductivity apparatuses. The current temperature limit for calibration-quality data sets for liquids is 500 K for nonelectrolytes [5]. No calibration-quality data sets are available for electrolytes. This makes it difficult to calibrate high-temperature thermal conductivity methods, especially those to be used for measurements on electrolytes. An excellent choice of fluid for standard-quality measurements is the sodium–potassium nitrate eutectic (54 mol% KNO_3). The eutectic melts at 495 K so that temperature continuity with the other standard data set is maintained. The eutectic has the additional advantage of having a larger liquid temperature range than either of the pure components and is usable to at least 773 K before significant decomposition of the melt occurs [6]. A second reason for studying the eutectic is its importance as a high temperature heat transfer fluid.

The apparatus constructed in this work was based on the liquid metal cell of Omotani et al. [2–4] but employed a two-capillary design to eliminate end effects and thus to obtain absolute measurements.

2. APPARATUS AND PROCEDURE

The apparatus consisted of four parts: a Wheatstone bridge circuit, a computer data acquisition system, a two-wire hot-wire cell, and a furnace. Except for the data acquisition system, each part was custom built.

The Wheatstone bridge circuit is shown in Fig. 1. The circuit includes

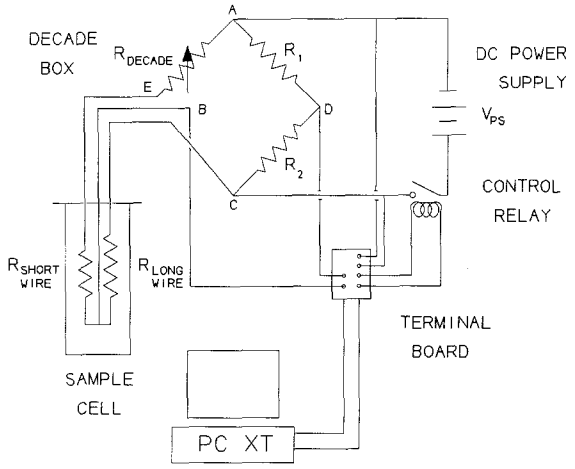

Fig. 1. Schematic diagram of the dual-wire cell.

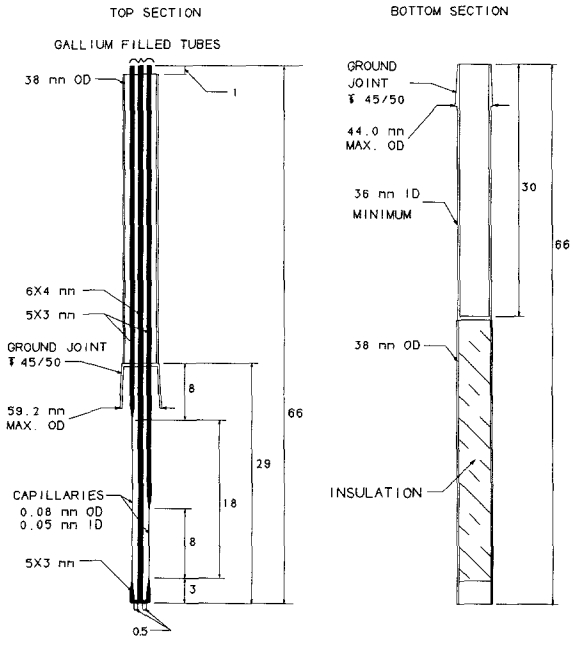

Fig. 2. Dual quartz capillary thermal conductivity cell.

a long and a short wire in opposite arms of the bridge. This configuration allows for the experimental elimination of end effects and makes absolute measurements possible.

The hot-wire cell is shown in Fig. 2. The cell was constructed of fused quartz (Quartz Scientific) in two sections which fit together via a ground joint. The bottom section was constructed from a 38-mm-O.D. tube to which was attached a 30-cm-long cylindrical sample container. Attached to the top of the sample container was the male end of a ground joint. Thermal insulation (Contronics) was placed inside the tube beneath the sample container. The top section was also constructed from a 38-mm-O.D. tube which was sealed at one end. Attached to the sealed end was the female end of a ground joint. Three smaller quartz tubes, two 5-mm-O.D. and one 6-mm-O.D., were fitted inside the top section. The 6-mm-O.D. tube was centered in the 38-mm-O.D. tube and extended through the glass seal at the bottom of the large tube into the sample container. This 6.0-mm-O.D. tube was split into a tee at its bottom, with the ends of the tee turned upward and drawn to a point to receive the bottom ends of the capillaries. The 5.0-mm-O.D. tubes were fitted midway between the center tube and the wall of the larger tube. Both of these tubes extended through the glass seal into the sample container and were drawn to a point to receive the top ends of the capillaries. One of the 5.0-mm-O.D. tubes extended farther into the sample container than the other to provide for two different length capillaries. One capillary space was about 18 cm long; the other, 8 cm. This resulted in an effective length of the hot wire of 10 cm. The capillaries were obtained by special order in 20-cm lengths (Wale Apparatus) with a nominal inside diameter of 50 μm and an outside diameter of 80 μm. The most troublesome aspect of the cell construction was the gluing of the capillaries into the supporting ends. Eventually, the problem was solved by using an adhesive (Cotronics, 905 Quartz Adhesive) to attach the capillaries to the pointed ends of the tubes. A moisture-proofing sealant (Cotronics, Duraseal 1529 UHT) was painted over the adhesive to prevent the molten salt from flowing through the adhesive. The maximum operating temperature of the sealant was about 1250 K according to the manufacturer. Thus the high-temperature limit of the apparatus was also about 1250 K because of possible degradation of the sealant. After the cell was constructed, the capillaries were filled with liquid gallium. Gallium freezes at 303 K and so sets the low-temperature limit of the apparatus. The gallium was introduced by pulling a vacuum on the two outer tubes while a funnel filled with gallium was attached via tygon tubing to the top of the center tube. After filling the cell with gallium, tungsten leads were then slipped down the tubes into the gallium reservoirs in each of the three tubes. Insulation was then fitted between the three glass tubes and the large

outer tube of the top section. Down the middle tube was placed a 1-mm type K thermocouple (Marlin) sheathed in fused quartz to measure the sample temperature. By moving the thermocouple up and down the central tube, the absence of an axial temperature gradient in the molten salt could be confirmed.

The furnace is shown with the hot-wire cell in Fig. 3. The furnace was constructed from a 76-cm-long × 25-cm-O.D. carbon steel pipe, with a flange welded at each end of the pipe. The ends of the pipe were fitted with end plates which had a groove machined for an o-ring. A 1.5-in. NPT threaded hole was machined in the middle of each end plate, and 1.5-in.

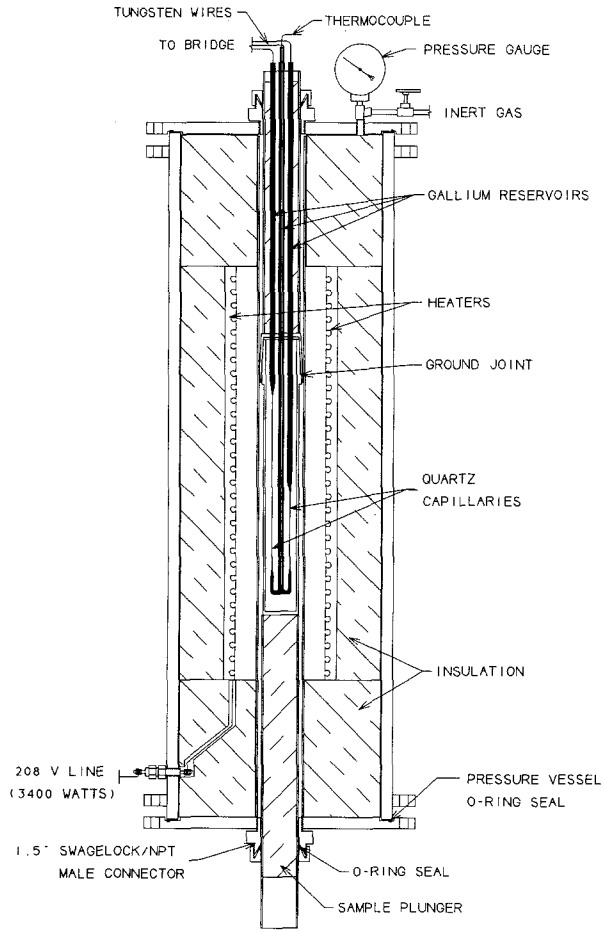

Fig. 3. Furnace with cell in place.

male connectors (Swagelock) were placed in these ports. The fittings were special ordered to be bored through. This allowed the 38-mm-O.D. tube of the thermal conductivity cell to slip easily through the fitting. By slipping an o-ring over the outside of the glass tube and reversing the ferrule inside the Swagelock fitting, it was possible to achieve a glass-to-metal seal. The reversed ferrule pressed the o-ring into the beveled part of the Swagelock fitting and against the outside of the glass tube wall. With both end plates bolted in place and both sections of the cell inserted through the Swagelock fittings, the furnace (pipe) was both pressure and vacuum tight. This was done to allow vacuum drying of the salts directly in the furnace and for the use of different atmospheres inside the furnace.

The arrangement of the heater and insulation inside the furnace is as follows. Three layers of 5-cm-thick insulation board (Fiberfax) were placed at the bottom, as were the power feed-throughs for the heating elements. The feed-throughs (Conax) were located about 5 cm above the bottom of the pipe. The insulation boards supported two 46-cm-long × 13-cm-O.D. semicylindrical heating elements (Lindberg). The heating elements were put together to form a tube and wrapped several times with a 1.3-cm-thick insulation blanket (Cotronics). The resulting thickness of the insulation layer around the heating elements was 5 cm. The blanket-covered elements were slipped into the pipe until the assembly rested on the insulation boards. Stacked on the heating elements were three more 5-cm-thick insulating boards. Down the center of the furnace, running from end plate to end plate, was a 5.1-cm-O.D. quartz tube. This tube acted as both a guide for mating the top and bottom sections of the hot-wire cell and a spill container. A 3-mm-I.D. × 5-mm-O.D. tube about 25 cm long was glued to the outside of the centering tube near the top of the furnace. This tube served as a guide for the type K thermocouple (Marlin) used by the controller. The furnace was controlled by a self-tuning PID controller (Omega 7000). Self-tuning was an important feature because of the wide range of temperatures encountered. The controller was used to turn on and off a solid-state relay and thus control the heating elements. It should be noted that the PID control was in time and not in power level. The furnace was allowed to stablize for 6 h until the temperature was constant to within ± 0.1 K. The large thermal mass of the salt helped to achieve this level of stablility.

The procedure for loading the sample was as follows. The top section of the cell was moved to the top of the furnace. The sample container was loaded with the solid salt and introduced into the furnace from the bottom. The sample container was slipped far enough into the furnace so that its bottom was at the same level as the bottom of the heating elements. Since the particular batch of salt used in our study packed poorly, it was

necessary to withdraw the sample cup and add more salt after the first batch had melted. Once the sample container was filled with molten salt, it was centered in the furnace. The top section was then lowered into the salt until the ground joint surfaces met. To secure the cell, the metal-to-glass seals were tightened by turning the nut on the 1.5-in. male connectors.

The bridge was powered by a Hewlett–Packard (Model 6213A) power supply used as a constant voltage source. The supply was used both to balance the bridge and to provide the power for heating. A Fluke multimeter (Model 8840A) was used to indicate a balanced condition in the bridge. A data acquisition system consisting of an IBM PC XT with an analog-to-digital converter card (Strawberry Tree ACPC-16) was used to read both the offset voltage V_o and the applied voltage V_a. The resistance of the central section of the long wire was then calculated from

$$R_w(t) = R_l - R_s = \frac{\left\{R_d\left[V_o + V_a\left(\frac{R_2}{R_1+R_2}\right)\right]\left[1-\frac{R_s}{R_l}\right]\right\}}{\left\{V_a - \left[V_o + V_a\left(\frac{R_2}{R_1+R_2}\right)\right]\left[1+\frac{R_s}{R_l}\right]\right\}} \tag{1}$$

where R_l and R_s are the resistances of the long and short wires, R_1 and R_2 are the resistances of the precision resistors, and R_d is the value of the decade resistor in the balanced condition. Typically, R_l was about 34 Ω, R_s about 20 Ω, and R_d about 14 Ω. Both R_1 and R_2 were 100.00 Ω. The ratio of R_s/R_l is given by

$$\frac{R_s}{R_l} = \frac{\rho L_s/A_s}{\rho L_l/A_l} = \frac{L_s \pi r_l^2}{L_l \pi r_s^2} = \frac{L_s r_l^2}{L_l r_s^2} \tag{2}$$

where ρ is the electrical resistivity of gallium, L_l and L_s the lengths, A_l and A_s the cross-sectional areas, and r_l and r_s the inside radii of the long and short capillaries, respectively. In practice, r_l and r_s were similar but not equal since the manufacturer guaranteed only a $\pm 10\%$ tolerance on the dimensions of the capillaries. The actual inside radius of the filaments was determined by measurement of the resistance of the capillaries. This was done using the accurate four-wire technique, which compensates for the resistance of the multimeter leads (Fluke 8840A). From the resistance, the resistivity of gallium, and the measured length of the filaments, the radius of the filament was determined. The outside radii of the filaments were measured with a microscope.

The temperature rise of the wire was calculated using the analysis developed by Kestin and Wakeham [7] for a dual-wire apparatus where the two wires have slightly different radii. The appropriate equations are

$$\Delta T_w(t) = \Delta T^*/(1+\varepsilon_5) \tag{3}$$

$$\Delta T^* = \frac{(R_l - R_s) - (R_l(0) - R_s(0))}{\kappa(R_l(0) - R_s(0))} \tag{4}$$

$$\Delta T^* = \frac{(R_l - R_s) - R_d}{(1/\rho)(d\rho/dt)\,\dot{R}_d} \tag{5}$$

$$\varepsilon_5 = \frac{R_s(0)\,\varepsilon_4}{R_d} \tag{6}$$

$$R_s(0) = \frac{R_d L_s A_l}{(L_l A_s - L_s A_l)} \tag{7}$$

$$\varepsilon_4 = \frac{\varepsilon[1 + \ln(4\alpha t/r_s^2 C)]}{\ln(4\alpha t/r_s^2 C)} \tag{8}$$

$$\varepsilon = 1 - \frac{\sigma_s}{\sigma_l} = 1 - \frac{R_s L_l}{R_l L_s} = 1 - \frac{A_l}{A_s} \tag{9}$$

where $\Delta T_w(t)$ is the temperature rise of the middle section of the long wire, $\kappa = (1/\rho)(d\rho/dt)$ is the temperature coefficient of the resistivity, C is the exponential of Euler's constant, σ_s and σ_l are the resistance per unit lengths for the short and long wire, respectively, and α is the thermal diffusivity of the fluid. The temperature rise calculated from this set of equations was then treated as outlined below in the analysis section.

It was also necessary to calculate the heat dissipated per unit length by the middle section of the long wire. This quantity was also derived by Kestin and Wakeham [7] as follows:

$$q_w = \frac{q(t)}{(1-\varepsilon_1)^2\,(1+\varepsilon_2)} \tag{10}$$

$$q(t) = \left[\overline{V_a(t)} \Big/ \left[\frac{\overline{(R_l - R_s)}}{(L_l - L_s)}(L_l + L_s) + R_d\right]\right]^2 \frac{\overline{(R_l - R_s)}}{(L_l - L_s)} \tag{11}$$

$$\varepsilon_1 = \frac{2\sigma_l \varepsilon L_l L_s}{(L_l - L_s)\,R_d + (R_l(0) - R_s(0))(L_l + L_s)} \tag{12}$$

$$\varepsilon_1 = \frac{\rho \varepsilon L_s}{A_l R_d} \tag{13}$$

$$\varepsilon_2 = \frac{L_s \varepsilon}{(L_l - L_s)} \tag{14}$$

where $\overline{R_l - R_s}$ and $\overline{V_a(t)}$ are the average values of these quantities taken

over the duration of the heating. The effect of wires having two different radii was taken into account.

The procedure for actually taking the measurements was as follows. After balancing the bridge, a computer program was run which closed the relay applying power to the bridge. The program then sampled the offset and applied voltages in turn. Two hundred samples were taken over a 3.4-s period. From these offset and applied voltages, the thermal conductivity was determined as outlined in the Analysis section. Each value of thermal conductivity reported below represents the average of five independent trials. The repeatability was within $\pm 1\%$ of the average value.

3. ANALYSIS

The model for the experiment is an infinite line source of heat submersed in an infinite fluid medium. By monitoring the temperature response of the wire to a step voltage input, the thermal conductivity of the fluid can be deduced. For an infinite line source of heat in an infinite fluid medium, the ideal temperature rise of the wire ΔT_{id} can be calculated using an expression derived by Carslaw and Jaegar [8] and Healy et al. [9] for $t \gg r_w^2/4\alpha$, where r_w is the radius of the filament and α is the thermal diffusivity of the fluid. The inequality is satisfied shortly after heating is started, that is, in the time interval $10\text{ ms} < t < 100\text{ ms}$. The expression is

$$\Delta T_{id} = T_w - T_w(0) = \frac{q}{4\pi\lambda} \ln\left(\frac{4\lambda t}{r_w^2 \rho C_p C}\right) \tag{15}$$

where T_w is the temperature of the wire, $T_w(0)$ the equilibrium temperature of the wire prior to heating, q the heat dissipation per unit length, λ the thermal conductivity, ρ the density, C_p the heat capacity, t the time from the application of the step voltage, and C is equal to $\exp(\gamma)$ where γ is Euler's constant. If it is assumed that all physical properties are independent of temperature over the small range of temperatures considered (ca. 2 K), then

$$\lambda = \frac{q}{4\pi(d\,\Delta T_{id}/d \ln t)} \tag{16}$$

where $d\,\Delta T_{id}/d \ln t$ is found experimentally from a plot of ΔT_{id} vs $\ln t$.

Healy et al. [9] also derived several corrections for the deviation of the model from reality. These may be written as

$$\Delta T_{id} = \Delta T_w(t) + \sum_i \delta T_i \tag{17}$$

where $\Delta T_w(t)$ is the measured temperature rise of the wire and δT_i are the

corrections to the temperature rise. δT_1 accounts for the finite physical properties of the wire and is given by Healy et al. [9] as follows:

$$\delta T_1 = \frac{r_w^2[(\rho C_p)_w - (\rho C_p)]}{2\lambda t} \Delta T_{id} - \frac{q}{4\pi\lambda} \frac{r_w^2}{4\alpha t}\left(2 - \frac{\alpha}{\alpha_w}\right) \tag{18}$$

where $(\rho C_p)_w$ is the volumetric heat capacity of the wire and α and α_w are the thermal diffusivity of the fluid and wire, respectively.

The correction due to the finite extent of the fluid is given by Healy et al. [9]:

$$\delta T_2 = \frac{q}{4\pi\lambda}\left(\ln\frac{4\alpha t}{b^2 C} + \sum_{v=1}^{\infty} \exp^{-g_v^2 \alpha t/b^2}[\pi Y_o(g_v)]^2\right) \tag{19}$$

where b is the inside diameter of the cell, Y_o is the zero-order Bessel function of the second kind, and g_v are the roots of J_o, the zero-order Bessel function of the first kind. Although the first several roots are readily available, the higher roots can be found to sufficient accuracy using an expression from the work of Watson [10]:

$$g_v = (\pi v - \pi/4) + \frac{1}{8(\pi v - \pi/4)} - \frac{31}{385(\pi v - \pi/4)^3} + \frac{3779}{15{,}366(\pi v - \pi/4)^5} \tag{20}$$

Values of Y_o can be calculated using the polynomial approximation given by Abramowitz and Stegun [11].

The effect of the insulating layer on the measurement has been evaluated analytically by Nagasaka and Nagashima [12]. The correction is given by

$$\delta T_3 = \frac{-q}{4\pi\lambda}\left[\ln\left(\frac{r_w}{r_l}\right)^2 + \frac{2\lambda}{\lambda_l}\ln\frac{r_l}{r_w} + \frac{\lambda}{\lambda_l} + A\right] \tag{21}$$

with

$$A = \frac{1}{t}(C_0 + B\ln t)$$

$$C_0 = C_1 + C_2 + B\ln\left(\frac{4\alpha}{r_l^2 C}\right)$$

$$C_1 = \frac{r_w^2}{8}\left[\left(\frac{\lambda - \lambda_l}{\lambda_w}\right)\left(\frac{1}{\alpha_w} - \frac{1}{\alpha_l}\right) + \frac{4}{\alpha_l} - \frac{2}{\alpha_w}\right]$$

$$C_2 = \frac{r_1^2}{2}\left(\frac{1}{\alpha} - \frac{1}{\alpha_l}\right) + \frac{r_w^2}{\lambda_l}\left(\frac{\lambda_l}{\alpha_l} - \frac{\lambda_w}{\alpha_w}\right)\ln\left(\frac{r_l}{r_w}\right)$$

$$B = \frac{r_w^2}{2\lambda}\left(\frac{\lambda_l}{\alpha_l} - \frac{\lambda_w}{\alpha_w}\right) + \frac{r_l^2}{2\lambda}\left(\frac{\lambda}{\alpha} - \frac{\lambda_w}{\alpha_w}\right)$$

where r_1, α_1, and λ_1 are the radius, thermal diffusivity, and thermal conductivity of the insulating layer. Implicit in this expression is the effect of the physical properties of the wire.

Radiation by the fluid can be accounted for using an analytical expression for the temperature rise of the wire given by Nieto de Castro et al. [13]:

$$\Delta T = \frac{q}{4\pi\lambda}\left(1 + \frac{Br_w^2}{4\alpha}\right)\ln\frac{4\alpha t}{r_w^2 C} + \frac{Bqr_w^2}{16\pi\alpha\lambda} - \frac{Bqt}{4\pi\lambda} \tag{22}$$

where B is the radiation parameter and is a measure of the contribution of radiant emission by the fluid to the heat transfer process. From Eq. (22) Nieto de Castro et al. [13] derived the following expression for the correction to the observed temperature rise:

$$\delta T_4 = \frac{-qB}{4\pi\lambda}\left(\frac{r_w^2}{4\alpha}\ln\frac{4\alpha t}{r_w^2 C} + \frac{r_w^2}{4\alpha} - t\right) \tag{23}$$

They used Eq. (22) to show that emission from a fluid causes the ΔT vs $\ln t$ slope to exhibit a slight curvature, concave to the $\ln t$ axis.

ΔT, after correction for the other effects mentioned, can be fit to Eq. (22) to obtain B as suggested by Nieto de Castro et al. [13]. Equation (23) can then be used to calculate δT_4.

The chief advantage of the transient hot-wire technique is its ability to eliminate the convection contribution to the thermal conductivity. The onset of convection causes the heat to flow away from the wire much more quickly than occurs by conduction, resulting in a temporary temperature drop in the wire. Such a drop is manifested by a curvature in the ΔT vs $\ln t$ plot. To verify the absence of convection, the residuals between the fitted line and the data are plotted as a function of time. If the residuals are evenly scattered about zero over the duration of the measurement, no convection is assumed to have occurred.

The final effect to be considered is that due to the finite length of the wire (end effects). This effect results in heat lost axially in the fluid and in the wire at the point where the wire is joined to the support leads. This effect is compensated for experimentally by using a long and a short wire in opposite arms of a resistance bridge. The key here is that the wire-to-support lead transitions be as geometrically similar as possible, so that the end effects are the same in both wires. The effective length of the wire is then the difference in length between the long and short wires.

The actual temperature at which the thermal conductivity is reported is the average temperature of the fluid during the heating process. That is,

$$T_R = T_o + \frac{\Delta T(t_I) + \Delta T(t_F)}{2} \tag{24}$$

where T_o is the temperature of the fluid at the start of a measurement, and t_I and t_F refer to the initial and final times of the data used to find the slope of ΔT vs $\ln t$, and the ΔT's are the temperatures of the wire at the corresponding times. In the case of an insulated wire, ΔT refers to the temperature at the surface of the insulation adjacent to the liquid. This temperature has been determined by Nagasaka and Nagashima [12] and is given by

$$\Delta T_i = \frac{q}{4\pi\lambda}\left[\frac{(P_3 + P_2 + P_1)}{t_i} + \ln\left(\frac{4\alpha t_i}{r_l^2 C}\right)\right] \tag{25}$$

with

$$P_3 = \frac{r_w^2}{4}\left(\frac{1}{\alpha_l} - \frac{1}{2\alpha_w}\right) + \frac{r_l^2}{4}\left(\frac{1}{\alpha} - \frac{1}{\alpha_l}\right)$$

$$P_2 = \frac{r_w^2}{2\lambda_l}\left(\frac{\lambda_l}{\alpha_l} - \frac{\lambda_w}{\alpha_w}\right)\ln\left(\frac{r_l}{r_w}\right)$$

$$P_1 = \ln\left(\frac{4\alpha t_i}{r_l^2 C}\right)\left[\frac{r_w^2}{2\lambda}\left(\frac{\lambda_l}{\alpha_l} - \frac{\lambda_w}{\alpha_w}\right) + \frac{r_l^2}{2\lambda}\left(\frac{\lambda}{\alpha} - \frac{\lambda_l}{\alpha_l}\right)\right]$$

where the subscript i refers to t_I or t_F.

In order to apply the temperature corrections, various physical properties were required. The electrical resistivity of gallium was obtained from the works of Pokorny and Astrom [14] and Ginter et al. [15]; the heat capacity of gallium from the works of Takahasi et al. [16], Amitin et al. [17], and Hultgren et al. [18]; and the density of gallium from the work of Koster et al. [19]. The thermal conductivity of gallium was given by Gamazov et al. [20]. The thermal conductivity and the heat capacity of quartz were obtained from the Thermophysical Properties Research Center compilations [21, 22]. For diethylene glycol, the densities were calculated from the correlation of Tawfik and Teja [23]; and the heat capacity from the ACS monograph on glycols [24]. The density and heat capacity of the $NaNO_3$–KNO_3 eutectic were obtained from Janz et al. [6].

4. SOURCE AND PURITY OF MATERIALS

The water used in this work was single distilled in our laboratory. The diethylene glycol was obtained from commercial sources and had a purity of 99% (Aldrich Chemical). The sodium and potassium nitrate were ACS Reagent grade (minimum purity, 99.5% for $NaNO_3$ and 99.8% for KNO_3) and were obtained from Fischer Scientific Co. The salts were dried

under vacuum at 473 K for several hours. The eutectic was prepared gravimetrically with a composition of 54.00 mol% KNO_3.

5. VALIDATION

In order to verify that the apparatus worked as expected, the thermal conductivity of water was measured. As found in our earlier work [25] on liquid metal probes, the thermal conductivity of water cannot be measured at temperatures above about 340 K using this technique. This is presumably because convection occurs much too rapidly and invalidates the measurement. Unfortunately, the other liquids for which standard data exist (toluene and dimethyl phthalate) dissolved the moisture-proofing layer used in the construction of the cell and so could not be used for testing. It was possible to measure the thermal conductivity of water only at a single temperature. The result obtained was $0.6494 \pm 0.5\%$ $W \cdot m^{-1} \cdot K^{-1}$ at 332.9 K. The IUPAC [5]-recommended value at this temperature is 0.6530 $W \cdot m^{-1} \cdot K^{-1}$, which is within 0.6% of our value. Since the cell was constructed of quartz, and the liquid metal is free to expand with temperature without changing the geometry of the cell, measurement at a single temperature is sufficient to verify the operation of the apparatus. Nevertheless, the thermal conductivity diethylene glycol was also measured to verify operation of our apparatus. The result at 334.0 K was $0.2015 \pm 0.2\%$ $W \cdot m^{-1} \cdot K^{-1}$. The result obtained previously [26] (by linear interpolation in temperature) was 0.2039 $W \cdot m^{-1} \cdot K^{-1}$, a difference of only 1%. The accuracy claimed for the earlier work [26] was 2.0%. Fischer [27] reported the thermal conductivity (by linear interpolation in temperature) to be 0.2023 $W \cdot m^{-1} \cdot K^{-1}$ at 334.0 K, a difference of only 0.4%. Moreover, Fischer claimed that his results were of calibration quality. These results, together with the availability of a complete mathematical description of the actual apparatus to eliminate biasing errors, demonstrate that the apparatus has no bias error and is limited only by its reproducibility.

6. RESULTS AND DISCUSSION

The thermal conductivity of the $NaNO_3$–KNO_3 eutectic (54.00 mol% KNO_3) was measured from 525 to 590 K. Each of the reported data points represents the average of five independent trials. The maximum deviation between the average and any individual trial was less than $\pm 1\%$. Thus, the repeatability of the apparatus was $\pm 1\%$, and by the discussion given above, the accuracy is also estimated to be $\pm 1\%$. The data are given in

Table I. The Thermal Conductivity of the $NaNO_3$–KNO_3 Eutectic (54.00 mol% KNO_3)

T(K)	λ ($W \cdot m^{-1} \cdot K^{-1}$)
526.2	0.4675 ± 0.44%
541.5	0.4650 ± 0.56%
557.5	0.4579 ± 0.60%
572.4	0.4543 ± 0.75%
588.0	0.4484 ± 0.94%

Table I and could be represented with an average deviation of 0.17% and a maximum devation of 0.3% by the equation

$$\lambda = 0.63496 - 3.1650 \times 10^{-4} T \tag{26}$$

where λ is in $W \cdot m^{-1} \cdot K^{-1}$ and T is in K. The data are plotted along with the work of Omotani et al. [2], Kitade et al. [28], and Tufeu et al. [29] in Fig. 4. These data sets were also selected by Nagasaka and Nagashima [1] after a critical review of the literature on these compounds. The data

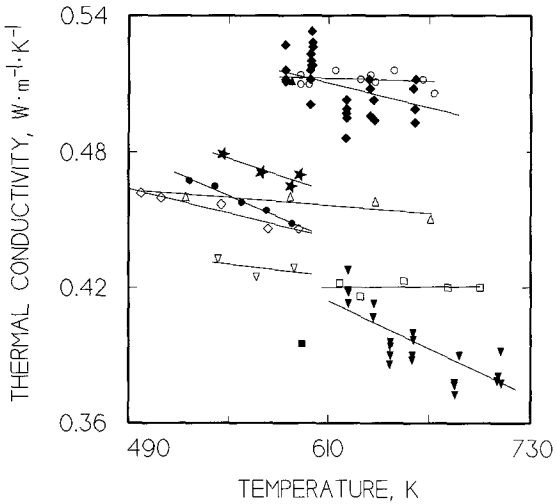

Fig. 4. The thermal conductivity of $NaNO_3$–KNO_3 mixtures: (●) 46 mol% $NaNO_3$, this work; (◆) $NaNO_3$ and (▼) KNO_3, Kitade et al. [28]; (○) $NaNO_3$, (△) 50 mol% $NaNO_3$, and (□) KNO_3, Tufeu et al. [29]; (▲) $NaNO_3$, (★) 75 mol% $NaNO_3$, (◇) 50 mol% $NaNO_3$, (▽) 30 mol% $NaNO_3$, and (■) 10 mol% $NaNO_3$, Omotani et al. [2].

of both Omotani et al. [2] and Kitade et al. [28] were measured using variants of the transient hot-wire technique. Omotani et al. [2] used a single capillary liquid metal probe. Since only a single wire was used, the technique was relative and utilized toluene as a calibration fluid. Kitade et al. [28] used a ceramic-coated platinum wire with potential leads at either end of the wire to eliminate end effects. Tufeu et al. [29] used the steady-state concentric cylinders technique. Because of differences in concentrations, direct comparison with the data of other investigators is not possible; only qualitative comparisons can therefore be made.

Several conclusions can be drawn from the results shown in Fig. 4. The first is that the results are about where they should be—more or less halfway between the results for pure $NaNO_3$ and those for pure KNO_3. The second conclusion is that the data obtained in this work show much less scatter than the data of the other workers. Finally, the slope of the data for the 54 mol% KNO_3, 46% $NaNO_3$ mixture is very similar to the slopes obtained by Kitade et al. for pure KNO_3 and $NaNO_3$. This is more evident in Fig. 5, where only the results of Kitade et al. [28] are plotted in addition to the results obtained in the present study.

During the course of this work, it was found that above 600 K the

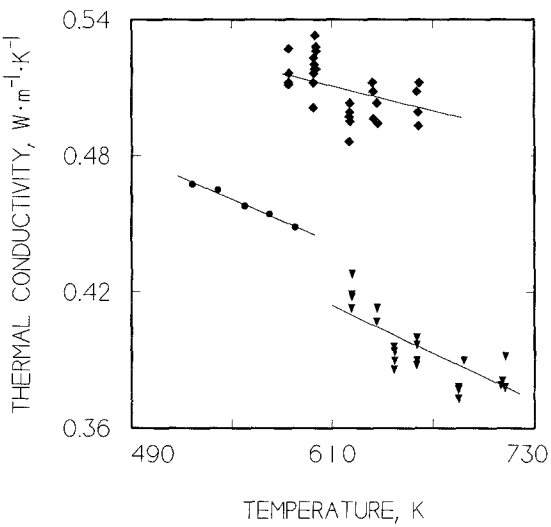

Fig. 5. The thermal conductivity of 54.00 mol% KNO_3–$NaNO_3$ measured in this work compared with the results of Kitade et al. [28] for the pure components: (●) 46 mol% $NaNO_3$, this work; (◆) $NaNO_3$ and (▼) KNO_3, Kitade et al. [28].

capillaries no longer properly insulated the gallium from the salt. When the insulation failed, current leaked through the salt and resulted in a thermal conductivity that was too high. Table I lists the maximum deviation from the average thermal conductivity at each temperature. The table shows that reproducibility gets worse with temperature. By 625 K, there was so much current leaking from one capillary through the salt and back into the second capillary that it was impossible to get any kind of temperature response curve. Nagasaka [30] believes that the quartz capillaries should retain their insulative capability up to about 650 K. An attempt was therefore made to measure the thermal conductivity of KNO_3 from 620 to 650 K. When the current was routed through both the long and the short wire (normal operation), it was impossible to get any temperature response from the filaments. The result was a thermal conductivity two orders of magnitude higher than expected. At first, the seals at the top and bottom of the capillaries were suspected of leaking. However, when each wire was used individually as the hot wire, the results were very reasonable and only about 15% higher than expected (as compared to the work of Kitade et al. [28]). The reproducibility was about $\pm 5\%$. This indicated that some problem still existed, but that it was not as severe as found with two wire operation. If the seals were leaking, the one-wire configuration should work no better than the two-wire configuration. Additionally, the seals were tested independently prior to cell construction by immersing a tungsten electrode in a tube filled with liquid gallium and sealed at the bottom according to the procedure discussed previously. The bottom of the tube was then immersed in a test tube containing molten KNO_3 for 48 h at 773 K. The test tube was removed while the salt was still molten and a second tungsten electrode was immersed in the molten salt. The resistance between the two electrodes was then measured and found to be greater than 20 MΩ. Based on these two tests, it was postulated that a current leak occurred from capillary to capillary at temperatures greater than about 600 K.

There appear to be two possibilities for extending the technique to higher temperatures. The first is to use thicker filaments. The second is to coat the filaments in order to plug the porous quartz structure. The second option offers a potentially higher temperature range and is recommended for further work. However, a suitable coating needs to be identified. This may seem to bring us back to the original problem of coating a wire, but there are differences. The first is that now the quartz base has a lower thermal expansion than any likely coating material. Instead of the insulation layer cracking because of expansion of the base metal, the layer will be compressed because its thermal expansion is greater than that of the base quartz. Second, as long as the quartz can insulate the gallium from the

pore plugging layer, the layer can be electrically conducting. Thus, two previous constraints on the insulating layer no longer exist.

7. CONCLUSIONS

For the first time, the transient hot-wire technique has been applied to the measurement of the thermal conductivity of electrolytes up to 590 K with an accuracy of $\pm 1\%$. The apparatus was used to measure the sodium–potassium nitrate eutectic up to 590 K. Although the apparatus was designed to go to 1373 K, the capillaries failed to insulate the gallium from the salt above 600 K. The problem can be solved by the use of an appropriate coating, although a coating has not been identified in this work.

ACKNOWLEDGMENTS

This work would not have been possible without the skill and patience of the glassblowers of Georgia Tech, Jerry Cloninger and Donald Woodyard. Discussions with Dr. Yuji Nagasaka of Keio University regarding his experiences with glass capillilary cells were very helpful. Financial support was provided by the Fluid Properties Research Institute, a consortium of companies engaged in the measurement and prediction of thermophysical properties of fluids.

REFERENCES

1. Y. Nagasaka and A. Nagashima, *Int. J. Thermophys.* **12**:769 (1991).
2. T. Omotani, Y. Nagasaka, and A. Nagashima, *Int. J. Thermophys.* **3**:17 (1982).
3. M. Hoshi, T. Omotani, and A. Nagashima, *Rev. Sci. Instrum.* **52**:755 (1981).
4. T. Omotani and A. Nagashima, *J. Chem. Eng. Data* **29**:1 (1984).
5. K. N. Marsh (ed.), *Recommended Reference Materials for the Realization of Physicochemial Properties* (Blackwell Scientific, Boston, 1987).
6. G. J. Janz, C. B. Allen, N. P. Bansal, R. M. Murphy, and R. P. T. Tomkins, *Physical Properties Data Compliations Relavant to Energy Storage. II. Molten Salts: Data on Single and Multicomponent Salt Systems*, Technical Report NSRDS-NBS-61-PT-2 (National Bureau of Standards, Washington, D.C.), 1979.
7. J. Kestin and W. A. Wakeham, *Physica* **92A**:102 (1978).
8. H. S. Carslaw and J. C. Jaeger, *Conduction of Heat in Solids*, 2nd ed. (Oxford University Press, London, 1959).
9. J. J. Healy, J. J. de Groot, and J. Kestin, *Physica* **82C**:392 (1976).
10. G. N. Watson, *A Treatise on the Theory of Bessel Functions*, 2nd ed. (Cambridge University Press, Cambridge, England, 1962).
11. M. Abramowitz and I. A. Stegun (eds.), *Handbook of Mathematical Functions* (Dover, New York, 1965).
12. Y. Nagasaka and A. Nagashima, *J. Phys. E Sci. Instrum.* **14**:1435 (1981).

13. C. A. Nieto de Castro, S. F. Y. Li, C. Maitland, and W. A. Wakeham, *Int. J. Thermophys.* **4**:311 (1983).
14. M. Pokorny and H. V. Astrom, *J. Phys. F* **6**:559 (1976).
15. G. Ginter, J. G. Gasser, and R. Kleim, *Phil. Mag. B* **54**:543 (1986).
16. Y. Takahashi, H. Kadokura, and H. Yokokawa, *J. Chem. Thermodyn.* **15**:65 (1983).
17. E. B. Amitin, Y. F. Minenkov, O. A. Nabutovskaya, I. E. Paukov, and S. I. Sokolova, *J. Chem. Thermodyn.* **16**:431 (1984).
18. R. Hultgren, P. D. Desai, D. T. Hawkins, M. Gleiser, K. K. Kelley, and D. D. Wagman, *Selected Values of the Thermodynamic Properties of the Elements* (American Society for Metals, Metals Park, OH, 1973).
19. Von H. Koster, F. Hensel, and E. U. Franck, *Berichte Bunsen-Gesellschaft* **74**:43 (1970).
20. A. A. Gamazov, A. I. Motsar, and A. G. Khotnyanskii, *Izv. Vyssh. Uchebn. Zaved. Fiz.* **22**:113 (1979).
21. Y. S. Touloukian and C. Y. Ho (eds.), *Thermal Conductivity of Nonmetallic Solids*, The Thermophysical Properties Research Center Data Series, Vol. 2 (Plenum Press, New York, 1972).
22. Y. S. Touloukian and C. Y. Ho (eds.), *Specific Heat of Nonmetallic Solids*, The Thermophysical Properties Research Center Data Series, Vol. 5 (Plenum Press, New York, 1972).
23. W. Tawfik and A. S. Teja, *Chem. Eng. Sci.* **44**:921 (1989).
24. G. O. Curme and F. Johnston (eds.), *Glycols* (Reinhold, New York, 1952).
25. R. M. DiGuilio, R. J. Lee, S. M. Jeter, and A. S. Teja, *ASHRAE Trans.* **96**:702 (1990).
26. R. DiGuilio and A. S. Teja, *J. Chem. Eng. Data* **35**:117 (1990).
27. S. Fischer, *Warme- und Stoffübertragung* **20**:183 (1986).
28. S. Kitade, Y. Kobayashi, Y. Nagasaka, and A. Nagashima, *High Temp. High Press.* **21**:219 (1989).
29. R. Tufeu, J. P. Petitet, L. Denielou, and B. Le Neindre, *Int. J. Thermophys.* **6**:315 (1985).
30. Y. Nagasaka, Personal communication (1991).